Design of Graphene-based Plasmonic Nano-antenna Arrays in the Presence of Mutual Coupling

Luke Zakrajsek*, Erik Einarsson*, Ngwe Thawdar†, Michael Medley† and Josep Miquel Jornet*

*Department of Electrical Engineering. University at Buffalo, The State University of New York, Buffalo, NY 14260, USA, E-mail: lukezakr, erikeina, jmjornet@buffalo.edu

†Air Force Research Laboratory/RITE, Rome, NY 13441, USA, Email: ngwe.thawdar, michael.medley@us.af.mil

***Abstract*—Graphene-based plasmonic nano-antennas are envisioned as an enabling component for compact communication systems in the Terahertz (THz) band (0.1-10 THz). Despite their high efficiency and due to their reduced size, the total radiation power of individual nano-antennas is expectedly very low. To overcome this limitation, plasmonic nano-antenna arrays are proposed. In this paper, the performance of such arrays is analyzed while taking into account mutual coupling effects. First, by utilizing coupled mode theory, the impact of mutual coupling on the nano-antenna response is modeled. Then, the array factor and total gain for nano-antenna arrays is derived. Extensive electromagnetic simulations are conducted to validate the developed models and provide numerical results. It is shown that a nano-array can provide significant gain in relation to only a single nano-antenna while still occupying a compact footprint.**

I. Introduction

Over the past decade, wireless data rates have risen dramatically due to technology advancements and shifts in the way people consume data. By one estimate, wireless data rates have roughly doubled every eighteen months over the past few decades [1]. However, we are closing in on the limits of our current wireless technologies. Millimeter wave solutions have dominated the discussions on future communication systems, but they are far from being able to support Tbps. One solution currently being investigated to solve this problem is Terahertz (THz)-band (0.1–10 THz) communication [2]. In the past, generation and detection of THz signals with compact devices was a major challenge, and this limited the use of the band for wireless communication. Today, new tools and new materials are enabling us to close this so-called THz gap.

Among others, one of the most promising methods to enable terahertz communications relies on the use of graphene-based nano-transceivers and nano-antennas. Graphene's unique electrical properties, such as high electrical conductivity, make it ideal for supporting extremely high frequency signals [3], [4]. In particular, graphene supports surface plasmon polariton (SPP) waves at THz frequencies [5], [6]. An SPP wave is a confined electromagnetic wave coupled to electric charges between a metal and a dielectric. Hybrid structures based on III-V semiconductor materials can be used to excite THz plasma waves on graphene [7], and graphene-based resonant plasmonic cavities can be utilized to efficiently radiate them [8]. The system works reciprocally in reception.

Nevertheless, there are several limitations in single-antenna systems that motivate the development of graphene-based nano-antenna arrays [9]. An array configuration would simultaneously solve some of the inherent roadblocks to THz communication while opening up many new possibilities. For one, single nano-antennas suffer from limited available output power due to their small size, which can be up to three magnitudes smaller than the size of current wireless communication antennas. In addition, the THz band itself introduces significant losses in the form of spreading losses and attenuation due to molecular absorption. A THz band array can alleviate these problems by producing huge increases in gain due to power amplification and/or beamforming. In addition, large arrays introduce the possibility to take advantage of Multiple-Input and Multiple-Output (MIMO) communication schemes for both beamforming and spatial multiplexing.

In the design of an array there are two equally important challenges. First, the individual antenna that serves as the basic element of the array must be designed. This has already been the subject of multiple works, starting with [10]. Since then there have been many studies concerning graphene antennas which investigate variations such as electrically tunable [11], reconfigurable [12], and beamforming antennas [13]. The second challenge is to determine how these individual elements should be placed relative to each other. Here mutual coupling concerns become just as important as individual design, as this determines how closely antennas can be placed and subsequently determines the size of the total array. Some works have been done in this area, but they are not sufficient or applicable to this case. For example, in [14] coupling is considered between graphene nanoribbons, but it does not consider how the distance between elements affects coupling strength and how it impacts system performance. Analysis is needed which considers coupling among nano-antennas.

In this paper, we first analyze the mutual coupling between graphene-based nano-antennas. A mathematical analysis is provided along with numerical simulation of a two element array, which focuses on how the strength of mutual coupling changes with respect to the separation distance. The second contribution is an investigation of the performance of nano-antenna arrays in terms of the achievable gain and directivity.

Approved for Public Release; Distribution Unlimited: 88ABW-2016-5655.

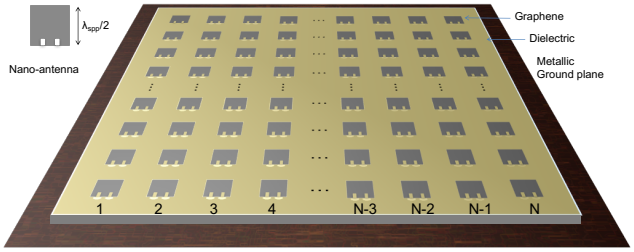

Fig. 1. Graphene-based plasmonic nano-antenna array.

In addition to the ideal gain, the impact of mutual coupling on the gain is considered. The analytical coupling model is validated by COMSOL Multiphysics simulations, which is also used to simulate performance of the array.

The rest of the paper is organized as follows. In Sec. II, we formulate a coupled mode theory model to investigate the mutual coupling between two elements, and we estimate the coupling coefficient which is mainly dependent on physical separation distance. In Sec. III, we discuss the performance of plasmonic nano-antenna arrays that takes into account the influence of the unique characteristics of a plasmonic array on gain and directivity. In Sec. IV, our theory is validated with simulation and numerical results. The coupling coefficient is found through simulation and the deterioration of the gain and directivity due to coupling is demonstrated. Using the simulation results, the achievable gain for an arbitrary number of elements is calculated. We conclude the paper in Sec. V.

II. Mutual Coupling Between Plasmonic Nano-Antennas

A. Coupled Mode Theory

The coupling between two resonant modes, such as those excited in resonant plasmonic nano-antennas, can be described mathematically using coupled mode theory. A full coupled mode model of the nano-antenna consists of a resonator with terms for conduction losses, radiation losses, and incident power from outside waves. From [14], the amplitude of the fields in two such nano-antennas is given by:

$$\frac{d\tilde{a}_1}{dt} = (i\omega_1 - \gamma_1 - \Gamma_1)\tilde{a}_1 + ik\tilde{a}_2 + i\sqrt{\gamma_1}(s_+ + i\sqrt{\gamma_2}e^{-ikd}\tilde{a}_2), \tag{1}$$

$$\frac{d\tilde{a}_2}{dt} = (i\omega_2 - \gamma_2 - \Gamma_2)\tilde{a}_2 + ik\tilde{a}_1 + i\sqrt{\gamma_2}(s_+ + i\sqrt{\gamma_1}e^{-ikd}\tilde{a}_1), \tag{2}$$

where a_1 and a_2 refer to the amplitudes and ω_1 and ω_2 are the natural frequencies [15]. In addition, γ is the radiative loss, Γ is the conduction loss, k is the coupling coefficient, s_+ is an incoming plane wave, and $\tilde{a}_{1,2} = a_{1,2}e^{j\omega t}$. While this is physically the case, when the goal is to investigate the near field coupling the model is greatly simplified by considering only the case of two lossless resonators. This is possible because the radiative and conductive losses are purely real, and therefore do not affect the resonance conditions induced by the reactive fields. In addition, when nano-antenna separation distances are small enough the near field coupling effects dominate and the coupling due to re-radiation of energy can be assumed to be zero [14]. Therefore, we assume that $\Gamma = 0$, $\gamma = 0$, and $s_+ = 0$, and that the resonators are excited by a time varying function. In this case, the equations for the resonators are given as:

$$\frac{da_1}{dt} = j\omega_1 a_1 + k_{12}a_2, \tag{3}$$

$$\frac{da_2}{dt} = j\omega_2 a_2 + k_{21}a_1. \tag{4}$$

The theory is valid as long as the coupling perturbations can be considered linear, which is true if the coupling terms $k_{12}a_2$ and $k_{21}a_1$ are much smaller than $j\omega_1 a_1$ and $j\omega_2 a_2$. Due to the symmetry of the problem, as well as energy conservation constraints discussed in [15], k_{12} must be equal to k_{21}. By taking this system of linear equations, one can solve for the eigenfrequencies, resulting in:

$$\omega = \frac{\omega_1 + \omega_2}{2} \pm \sqrt{\left(\frac{\omega_1 - \omega_2}{2}\right)^2 + |k_{12}|^2}, \tag{5}$$

where all the terms have been previously defined.

Physically the eigenfrequencies can be understood as the natural resonant frequencies of the two nano-antennas. Because a nano-antenna is a passive component, if the natural resonance frequency changes the result is not that the antenna will change operating frequency, but rather that it will now only radiate efficiently at the new resonances. In a system where the nano-antennas are already being exciting by a driving frequency, a change in the natural resonance will manifest itself as a change in the input impedance of the system. A typical array will be excited with the same frequency in each antenna. In this case, $\omega_1 = \omega_2 = \omega_0$, and the equation for the eigenfrequencies simplifies to

$$\omega = \omega_0 \pm k, \tag{6}$$

where k is the coupling coefficient.

B. Coupling Coefficient

The coupling coefficient is the result of the non-radiating near fields in the antenna and in conventional microstrip antenna theory it is derived from Maxwell's equations. There have been multiple attempts to model the mutual coupling between elements by using the transmission line model [16], the cavity model [17] [18] [19], or the method of moments for microstrip antennas. While these studies have had success in predicting coupling in metallic microstrip antennas, they have drawbacks which limit their use in studying coupling between plasmonic nano-antenna arrays. The problem is that most studies neglect surface waves to simplify the model. In a plasmonic nano-antenna, surface waves are critical to the operation of the antenna, and in fact are the only kind of waves that can be supported [8]. Even when studies account for surface waves, these surface waves are fundamentally different from SPP waves. The surface waves on metallic antennas occur at dielectric-dielectric boundaries and propagate over

the entire dielectric surface. These waves detract from the total power available to be radiated. In contrast, a plasmonic nano-antenna relies on SPP waves for generating the electric field and are only supported on the boundary between a dielectric and a metal, which means they can only exist where the patch is present. Because of these differences, the models used for predicting the coupling coefficient in metallic antenna arrays cannot be assumed to work for plasmonic arrays. Further analysis is needed which takes into account the properties of SPP waves.

Because the wavelength in a plasmonic nano-antenna is confined to a much smaller length than the radiated free space wavelength, it is expected that the mutual coupling will only start to become a major factor at distances related to the plasmonic wavelength, and consequently allow array elements to be separated much less than would be required in a perfect electric conducting antenna. Taking this into consideration, we predict that the coupling coefficient can be approximated by an exponential function given as

$$k = \alpha\omega_0 e^{-d\beta}, \tag{7}$$

where ω_0 is the resonant frequency without coupling, α and β are tuning constants, and d is the separation distance between elements.

III. Performance of Plasmonic Nano-antenna Arrays

In the design of an array, it is important to consider the overall system performance and how it is impacted by coupling and other factors. An array constructed using graphene nano-antennas will differ in two important aspects from a conventional array. First, as previously discussed, the coupling is expected to be based mainly on the physical size of the nano-antenna. For a plasmonic nano-antenna where there is a high confinement factor, near field coupling will only be an issue at distances much less than the free space wavelength. On one hand, this will allow for array elements to be placed much closer in proximity to each other, resulting in a high density of elements in the available area. On the other hand, this limits the beamforming abilities, which require distance comparable to the free space wavelength in order to achieve constructive superposition of field amplitudes. Second, the possibility to use one plasmonic signal source per antenna to power every element individually means that an increase in output power, and consequently gain, can be achieved independently of phase variation or beamforming. These differences are illustrated by considering the array factor $\mathcal{AF}$ of a uniform square planar array with N powered elements per side, separated by a distance of λ, which is given in [20] by

$$\mathcal{AF}(\theta,\phi) = \left(\frac{\sin\left(N\frac{\psi_x}{2}\right)}{\sin\left(\frac{\psi_x}{2}\right)}\right)\left(\frac{\sin\left(N\frac{\psi_y}{2}\right)}{\sin\left(\frac{\psi_y}{2}\right)}\right), \tag{8}$$

$$\psi_x = kd\sin\theta\cos\phi - \frac{2\pi}{kd}\sin\theta_0\cos\phi_0, \tag{9}$$

$$\psi_y = kd\sin\theta\sin\phi - \frac{2\pi}{kd}\sin\theta_0\sin\phi_0, \tag{10}$$

where θ refers to the elevation angle, ϕ is the azimuth, (θ_0,ϕ_0) is the beam pointing direction, $k = \frac{2\pi}{\lambda}$ is the wavenumber, and d is the uniform distance between elements. In a conventional array $\mathcal{AF}$ is normalized with respect to N to account for the total power being split between N antennas, and to better illustrate radiation pattern changes from field multiplication. However, here it is left unnormalized with respect to N due to the fact that the nano-antennas will be powered independently and contribute to the overall gain. In addition, for a plasmonic nano-antenna array the distance between the elements will be the plasmonic wavelength rather than some multiple of the freespace wavelength. In this case, we replace d with the plasmonic wavelength λ_{spp}, and the array factor becomes

$$\mathcal{AF}(\theta,\phi) = \left(\frac{\sin\left(N\frac{\psi_x}{2}\right)}{\sin\left(\frac{\psi_x}{2}\right)}\right)\left(\frac{\sin\left(N\frac{\psi_y}{2}\right)}{\sin\left(\frac{\psi_y}{2}\right)}\right), \tag{11}$$

$$\psi_x = \frac{2\pi}{\gamma}\sin\theta\cos\phi - \frac{2\pi}{\gamma}\sin\theta_0\cos\phi_0, \tag{12}$$

$$\psi_y = \frac{2\pi}{\gamma}\sin\theta\sin\phi - \frac{2\pi}{\gamma}\sin\theta_0\sin\phi_0, \tag{13}$$

where γ is the confinement factor and is equal to $\frac{\lambda}{\lambda_{\mathrm{spp}}}$. When using this formula it is clear that the higher the confinement factor becomes, the lower the directivity will be, although it still has a minimum value of 1. However, analysis using this formula suggests that even with decreased directivity due to a high confinement factor, or equivalently, close element spacing, the attainable gain is still high due to power multiplication.

IV. Simulation and Numerical Results

In this section, the analytical model for the mutual coupling coefficient is validated, and the nano-antenna array performance claims are verified by means of full-wave electromagnetic simulations. In order to numerically find the coupling coefficient, a two element array is simulated using COMSOL Multiphysics. Graphene is modeled as a transition boundary condition with complex-valued dynamic conductivity given by the model in [21], where $\tau_g = 0.5$ ps is the relaxation time of electrons in graphene, $T = 300$ K is the temperature, and with E_F values from 0.1 to 1.25 eV, where E_F is the Fermi energy of the graphene patch. These values are based on analysis of Raman spectra obtained from CVD-grown graphene. The graphene layer rests on top of a 90-nm-thick SiO_2 dielectric ($\epsilon_r = 4$), which separates the graphene from the ground plane. This thickness is chosen because it maximizes visual detection of graphene on SiO_2. The antenna is fed with a lumped port that connects the graphene layer to the ground plane on one side. A perfectly matched layer and scattering boundary are used to accurately approximate an infinite space. The antennas are meshed with a resolution of $\lambda_{spp}/5$. To simulate the array performance measures of gain and directivity, the same parameters are used to construct a uniform planar three by three array for a total of nine elements.

A. Validation of Mutual Coupling

The effect of mutual coupling on resonant frequency was found through the measurement of the input impedance at the ports. As previously discussed, the frequency at which the imaginary part of the input impedance disappears is considered to be the resonant frequency. The mutual coupling dependency on the separation of the elements was found by performing a frequency sweep for different separation distances for three different frequencies that are representative of the THz band. The coupling coefficient (7) was also plotted using curve fitting tools to match the tuning parameters. As shown in Fig. 2, the change in frequency as a function of separation distance is comparable to the plasmonic wavelength, which in this case is 2 μm for both simulations. It also shows that the matched coupling coefficient equations are well matched to their respective coupling sweeps. Table I summarizes the matched coefficients for each frequency.

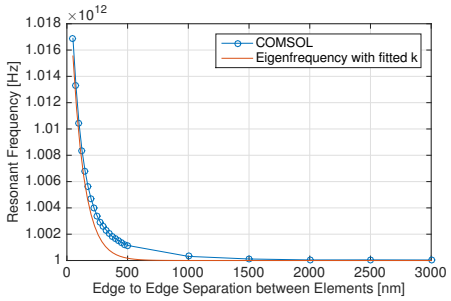

(a) Plasmonic Array Resonant Frequency at 1 THz

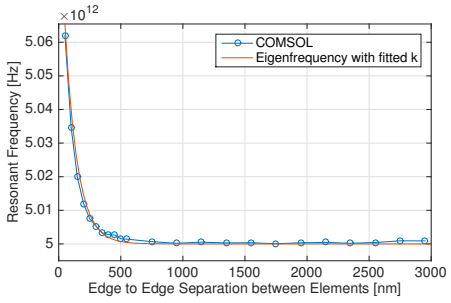

(b) Plasmonic Array Resonant Frequency at 5 THz

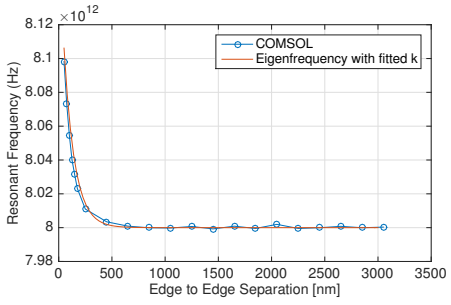

(c) Plasmonic Array Resonant Frequency at 8 THz

Fig. 2. Resonance frequency as a function of the separation distance between resonant elements for different antenna resonant frequencies.

TABLE I
CURVE FITTED PARAMETERS FOR k

Frequency	1 THz	5 THz	8 THz
α	0.02563	0.02158	0.02188
β	$1e10^{-11}$	$1e10^{-11}$	$1e10^{-11}$

B. Analysis of Array Performance

In addition to studying the change in frequency in a two element array, the overall array performance and the impact of mutual coupling on this performance was simulated. The simulation used a nine element array, and directivity and gain are calculated from radiated power values computed by COMSOL. The directivity as plotted in Fig. 3a takes into account the combined effects of the array directivity and the single nano-antenna's directivity, while neglecting power amplification. What can be seen from the graph is that the directivity when the antenna separation distance is comparable to λ_{spp} is predominately due to the directivity of the single nano-antenna, which is about 6.5 dB. The added directivity from the array due to constructive interference does not occur until the separation approaches $\lambda/2$. In Fig. 3b, the power multiplication gain of the array over that of a single nano-antenna is plotted. This gain in power is shown to be equal in magnitude to the square of the array factor, which for an array of nine elements is equivalent to 81, or about 19 dB. In both figures it is clear that mutual coupling effects cause a large drop in both directivity and power gain, but only for very close separation distances.

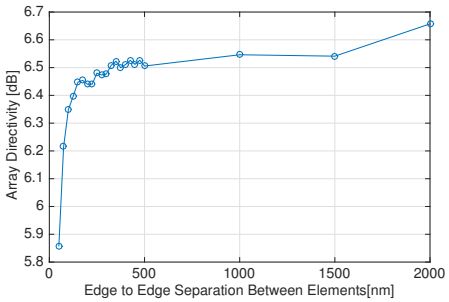

(a) Plasmonic Array Directivity at 8 THz

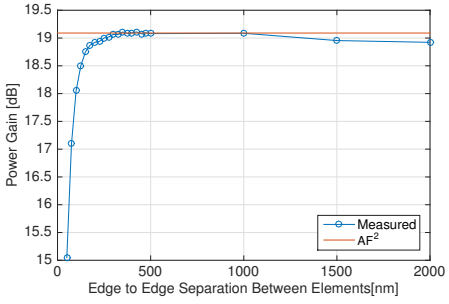

(b) Plasmonic Array Power Gain at 8 THz

Fig. 3. Directivity and power gain of a nine antenna uniform planar array as functions of the separation between elements.

Finally, in Fig. 4, the total gain of a plasmonic array is calculated based on the number of antennas in the array for different separation distances. The total gain shown here represents the maximum radiated power of a plasmonic array compared to that of a single isotropic nano-antenna and includes the directivity of a graphene nano-antenna, the directivity of the array, and the power multiplication from multiple powered antennas. It is important to note that even the lowest separation distance shown here is large enough that mutual coupling effects are not a concern.

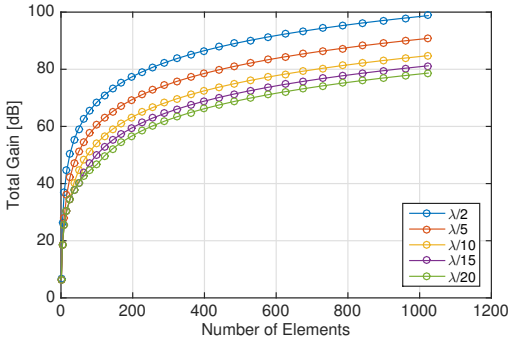

Fig. 4. Total gain of a graphene-based plasmonic nano-antenna array, as a function of the number of elements.

V. Conclusion

In this paper, the performance of graphene-based plasmonic nano-antenna arrays at THz frequencies has been analyzed by taking the impact of mutual coupling into account. Coupled mode theory has been utilized to model the mutual coupling between two neighboring plasmonic nano-antennas and the coupling coefficient has been defined. The resulting gain of an active plasmonic nano-antenna array has been derived, and finite-element simulations have been utilized to both validate the models and numerically explore the performance of plasmonic nano-antenna arrays. It has been shown that near field coupling between antennas becomes negligible at separation distances much less than the free space wavelength. Consequently, a very large number of elements can be integrated in plasmonic nano-antenna arrays with a resulting very small footprint and, potentially, lead to practical THz communication systems.

VI. Acknowledgement of Support and Disclaimer

(a) The State University of New York at Buffalo acknowledges the U.S. Government's support in the publication of this paper. This material is based upon work funded by AFRL, under AFRL Grant No. FA8750-15-1-0050.

(b) Any opinions, findings and conclusions or recommendations expressed in this material are those of the author(s) and do not necessarily reflect the views of AFRL.

References

[1] S. Cherry, "Edholm's law of bandwidth," *IEEE Spectrum*, vol. 41, no. 7, pp. 58 – 60, Jul. 2004.

[2] I. F. Akyildiz, J. M. Jornet, and C. Han, "Terahertz band: Next frontier for wireless communications," *Physical Communication (Elsevier) Journal*, vol. 12, pp. 16 – 32, Sep. 2014.

[3] K. S. Novoselov, V. Fal, L. Colombo, P. Gellert, M. Schwab, K. Kim *et al.*, "A roadmap for graphene," *Nature*, vol. 490, no. 7419, pp. 192–200, 2012.

[4] A. C. Ferrari, F. Bonaccorso, V. Fal'Ko, K. S. Novoselov, S. Roche, P. Bøggild, S. Borini, F. H. Koppens, V. Palermo, N. Pugno *et al.*, "Science and technology roadmap for graphene, related two-dimensional crystals, and hybrid systems," *Nanoscale*, vol. 7, no. 11, pp. 4598–4810, 2015.

[5] L. Ju, B. Geng, J. Horng, C. Girit, M. martin, Z. Hao, H. Bechtel, X. Liang, A. Zettl, Y. R. Shen, and F. Wang, "Graphene plasmonics for tunable terahertz metamaterials," *Nature Nanotechnology*, vol. 6, pp. 630–634, Sep. 2011.

[6] F. H. L. Koppens, D. E. Chang, and F. J. Garcia de Abajo, "Graphene plasmonics: a platform for strong light matter interactions," *Nano Letters*, vol. 11, no. 8, pp. 3370–3377, Aug. 2011.

[7] J. M. Jornet and I. F. Akyildiz, "Graphene-based plasmonic nano-transceiver for terahertz band communication," in *Proc. of European Conference on Antennas and Propagation (EuCAP)*, 2014.

[8] ——, "Graphene-based plasmonic nano-antenna for terahertz band communication in nanonetworks," *IEEE JSAC, Special Issue on Emerging Technologies for Communications*, vol. 12, no. 12, pp. 685–694, Dec. 2013.

[9] I. F. Akyildiz and J. M. Jornet, "Realizing ultra-massive mimo (1024× 1024) communication in the (0.06–10) terahertz band," *Nano Communication Networks*, vol. 8, pp. 46–54, 2016.

[10] J. M. Jornet and I. F. Akyildiz, "Graphene-based nano-antennas for electromagnetic nanocommunications in the terahertz band," in *Proc. of 4th European Conference on Antennas and Propagation, EUCAP*, Apr. 2010.

[11] I. Llatser, C. Kremers, A. Cabellos-Aparicio, J. M. Jornet, E. Alarcon, and D. N. Chigrin, "Graphene-based nano-patch antenna for terahertz radiation," *Photonics and Nanostructures - Fundamentals and Applications*, vol. 10, no. 4, pp. 353–358, Oct. 2012.

[12] M. Tamagnone, J. S. Gomez-Diaz, J. R. Mosig, and J. Perruisseau-Carrier, "Reconfigurable terahertz plasmonic antenna concept using a graphene stack," *Applied Physics Letters*, vol. 101, no. 21, p. 214102, 2012.

[13] M. Aldrigo, M. Dragoman, and D. Dragoman, "Smart antennas based on graphene," *Journal of Applied Physics*, vol. 116, no. 11, 2014.

[14] W. Tan, Y. Sun, Z.-G. Wang, and H. Chen, "Manipulating electromagnetic responses of metal wires at the deep subwavelength scale via both near-and far-field couplings," *Applied Physics Letters*, vol. 104, no. 9, p. 091107, 2014.

[15] H. A. Haus, *Waves and fields in optoelectronics*. Prentice-Hall,, 1984.

[16] E. Van Lil and A. Van de Capelle, "Transmission line model for mutual coupling between microstrip antennas," *IEEE Transactions on antennas and propagation*, vol. 32, no. 8, pp. 816–821, 1984.

[17] M. Malkomes, "Mutual coupling between microstrip patch antennas," *Electronics Letters*, vol. 18, pp. 520–522, 1982.

[18] E. Penard and J.-P. Daniel, "Mutual coupling between microstrip antennas," *Electronics Letters*, vol. 18, pp. 605–607, 1982.

[19] A. Derneryd, "A theoretical investigation of the rectangular microstrip antenna element," *IEEE Transactions on Antennas and Propagation*, vol. 26, no. 4, pp. 532–535, 1978.

[20] C. A. Balanis, *Antenna theory: analysis and design*. John Wiley & Sons, 2005.

[21] L. Zakrajsek, E. Einarsson, N. Thawdar, M. Medley, and J. M. Jornet, "Lithographically defined plasmonic graphene antennas for terahertz-band communication," *submitted for journal publication*, 2015.